systems

MDPI

Article

Intelligent Multi-Objective Optimization on Ship Lock Scheduling Considering Energy Consumption and Resource Constraints

Qi Xu [1,*], Jiahao Wang [2], Hongcheng Li [1], Song Wu [3,4,*] and Qiang Yan [3,4]

[1] School of Architecture and Transportation Engineering, Guilin University of Electronic Technology, Guilin 541004, China
[2] Guangxi Key Laboratory of ITS, Guilin University of Electronic Technology, Guilin 541004, China
[3] Pinglu Canal Group Co., Ltd., Nanning 530022, China
[4] Guangxi Laboratory of Modern Canal, Nanning 530004, China
* Correspondence: xuqi@guet.edu.cn (Q.X.); ncpclem372125562@163.com (S.W.)

Abstract

In response to the increasing operational complexity of inland waterway systems, this study develops a multi-objective optimization framework for ship lock scheduling under energy-consumption and resource constraints. The model evaluates five operational dimensions, namely average waiting time, lock utilization, total energy consumption, arrival rescheduling rate, and berth-overcapacity penalty. Based on historical lockage records from the Da Teng Gorge Ship Lock Hub, four representative multi-objective algorithms—NSGA-II, NSGA-III, MOEA/D, and SPEA-II—are comparatively examined. The revised analysis emphasizes trade-off performance rather than unsupported absolute dominance claims: NSGA-III shows the most balanced overall behavior on the preserved empirical instance, MOEA/D remains competitive in time-sensitive scenarios, and SPEA-II performs well in some overcapacity-control settings. To improve methodological transparency, the paper clarifies the physical meaning and source of major parameters, distinguishes measured quantities from scenario settings, and reports carbon impact as a derived indicator linked to energy consumption. These revisions provide a more transparent and practically interpretable basis for intelligent ship lock scheduling under congestion, energy, and resource constraints.

Keywords: ship lock scheduling; multi-objective optimization; lock utilization; energy consumption; berth-overcapacity control; inland waterway transport

Check for updates

Academic Editor:
Wen-Chyuan Chiang

Received: 18 March 2026
Revised: 26 April 2026
Accepted: 1 May 2026
Published: 3 May 2026

Copyright: © 2026 by the authors. Licensee MDPI, Basel, Switzerland. This article is an open access article distributed under the terms and conditions of the Creative Commons Attribution (CC BY) license.

1. Introduction

1.1. Research Background

Inland waterways serve as vital multimodal transport corridors, fostering regional economic integration through their strategic connectivity of industrial clusters, metropolitan hubs, and international ports. As a critical component of national infrastructure systems, these waterways leverage the intrinsic advantages of fluvial transportation—notably superior energy efficiency and exceptional bulk cargo capacity. Such characteristics have cemented their status as a sustainable freight solution, currently handling 47% of global bulk commodity movements, according to UNCTAD 2023 statistics. The ongoing optimization of lockage efficiency and channel standardization further amplifies their competitiveness within modern supply chain networks.

Take the Da Teng Gorge Ship Lock Hub as the research background. The ship lock is located in the core navigation section of the West River mainstem in China and serves as a critical water transport node along the Pearl River-West River Economic Corridor. It has long faced significant constraints due to high-intensity operations. With the continuous growth of regional water transport demand, the hub frequently experiences severe congestion during peak navigation periods, characterized by vessels lingering for extended periods before the ship lock, significantly delaying passage efficiency [1–3]. Although the hub is a large-scale water engineering facility with sufficient design redundancy for navigation capacity, current operational conditions, where actual transport volumes far exceed original design expectations, have resulted in consistently suboptimal lock utilization efficiency and ineffective realization of its cyclic performance potential. Such structural contradictions lead to efficiency losses across the entire water transport system and undermine the stability of regional supply chains, particularly in the construction materials sector.

Currently, management authorities are attempting to alleviate navigation pressure through a "dual-track" strategy, combining infrastructure expansion with intelligent scheduling optimization. However, from the perspectives of engineering geological conditions and capital investment, constructing large-scale parallel locks in a typical karst terrain environment poses extremely high technical complexity and fiscal burdens, making it difficult to implement effective expansion in the short term. Additionally, the current scheduling mechanism has shortcomings in terms of allocation logic and operational efficiency. The use of lock chambers and navigation channels exhibits high dwell times and low turnover rates, not only suppressing system operational efficiency but also exacerbating energy consumption and carbon emissions, thereby adversely affecting the development of green shipping within the region.

Therefore, the implementation of an intelligent scheduling framework that integrates real-time ship lockage data and multi-objective optimization techniques—particularly focusing on environmental and efficiency improvements—has emerged as a critical necessity.

1.2. Literature Review

Under this context, research on inland waterway navigation management, especially the ship lock scheduling problem (LSP), has become an important topic in transportation systems and maritime logistics. Recent studies show that the literature is evolving along several connected streams, including lock scheduling and co-scheduling, disturbance-aware and appointment-based scheduling, green and low-carbon optimization, data-driven maritime decision support, and multi-objective solution methodologies. Compared with earlier studies that focused primarily on chamber arrangement or local sequencing, newer research increasingly emphasizes integrated decision-making under congestion, uncertainty, environmental pressure, and inter-facility coordination.

In the field of lock scheduling and coordinated operation, Ji et al. [4] developed an adaptive large neighborhood search framework for the generalized lock scheduling problem, showing that large-scale lockage decisions can be solved effectively by tailored heuristics. Deng et al. [5] further examined inland-waterway lock congestion from the perspective of bottleneck theory and introduced a service-time-window model to capture temporal queuing dynamics. Zhao et al. [6] extended the problem to the co-scheduling of ship lifts and ship locks at the Three Gorges Dam, indicating that coordinated decisions across multiple navigation facilities are crucial for reducing system-wide delay. Ji et al. [7] then proposed a decomposition-based solution framework for the generalized serial-lock scheduling problem, significantly strengthening the methodological basis for solving large-scale serial-lock systems. More recently, Zhang et al. [8] investigated optimal scheduling in inland waterways with serial locks using mixed-integer linear programming, showing

that large-scale serial-lock coordination can be addressed more rigorously in modern optimization settings.

Another notable trend is that recent studies no longer assume perfectly punctual arrivals or static operating environments. Liu et al. [9] studied ship appointment scheduling for lockage operations with non-punctual arrivals and explicitly modeled appointment adjustment and ship rescheduling. Liu et al. [10] further addressed the ship scheduling problem based on channel-lock coordination in flood season, where water discharge variation, anchorage release timing, and coordinated allocation of channel and lock resources must be considered simultaneously. Gao et al. [11] proposed a congestion mitigation strategy based on a multi-objective moment bottleneck model, further highlighting the importance of dynamic traffic management under highly congested inland-waterway conditions. In addition, Li et al. [12] evaluated lock navigation scheduling rules from the perspective of multiple stakeholders, suggesting that fairness, safety, and resilience should also be considered when assessing operational strategies. These studies indicate that practical lock scheduling is increasingly disturbance-aware, appointment-sensitive, and connected with upstream and downstream traffic organization rather than limited to chamber-level sequencing alone.

At the same time, green and low-carbon objectives have become a central issue in inland waterway optimization. Zheng et al. [13] studied an energy-efficient lock group co-scheduling problem with ship lifts and approach channels, showing that system-level energy objectives can be integrated with coordinated navigation decisions. From a broader inland-waterway perspective, Golak et al. [14] presented a local-search heuristic for optimizing fuel consumption on inland waterway networks, while Defryn et al. [15] showed that skipper collaboration and joint speed optimization can improve inland-waterway efficiency. Tadeusz et al. [16] evaluated the impact of various trajectory simplification methods on the accuracy of ship CO_2 emission modeling. Jaewon et al. [17] developed a statistical prediction model for CO_2 emissions based on engine speed under various ship telegraph modes, and compared it with life cycle assessment (LCA) simulation results. Yang et al. [18] analyzed the optimal scheduling of vessels passing a waterway bottleneck by jointly considering delay and bunker-cost trade-offs, and Buchem et al. [19] explored vessel velocity decisions under uncertainty. Zhang et al. [20] further proposed an optimization method for ship transport capacity structure to alleviate inland-waterway traffic congestion. Taken together, these studies confirm that energy consumption, fuel cost, and CO_2-related concerns are now key criteria in modern navigation optimization, although relatively few studies simultaneously consider green objectives, lock resource constraints, and hub-level operational variability within one unified framework.

A further emerging direction is the combination of scheduling optimization with data analytics and systems-oriented decision support. Kweon et al. [21] used logical analysis of data to identify demurrage patterns and hidden inefficiencies in port operations, showing that real operational data can reveal congestion mechanisms that are difficult to detect using optimization models alone. Woo et al. [22] proposed a real-time-data-driven multi-objective decision framework in another application domain, offering a useful methodological analogy for dynamic decision support under uncertainty. Homayouni et al. [23] reviewed how digital twins can support sustainability-oriented seaport operations, indicating that smart maritime systems are moving toward integrated monitoring, scenario simulation, and optimization. Chen and Cheng [24] analyzed the broader economic consequences of inland waterway disruptions in a changing climate, reminding researchers that lock congestion and failures can have impacts far beyond local operations. Calderón-Rivera et al. [25] also reviewed sustainable inland waterway transport from a wider systems perspective.

This broader literature helps position ship lock scheduling within the context of smart and resilient maritime infrastructure rather than as an isolated optimization problem.

From the perspective of solution methodology, recent developments in multi-objective optimization also provide important support for ship lock scheduling research. Liu et al. [26] proposed a convergence-diversity balanced fitness evaluation mechanism for decomposition-based many-objective optimization, improving the trade-off between solution quality and population diversity. He et al. [27] developed a dynamic reference-point-based fuzzy relative entropy mechanism for energy-efficient scheduling, illustrating how advanced fitness design can improve many-objective search performance. Li et al. [28] more recently proposed an ensemble of neighborhood search operators for decomposition-based multi-objective evolutionary optimization, reflecting the current trend toward adaptive and hybridized search strategies. These developments are highly relevant because ship lock scheduling with waiting time, utilization, energy use, congestion mitigation, and resource constraints is essentially a complex multi-objective decision problem.

Based on the above review, several research gaps can be identified. First, although recent lock scheduling studies have substantially improved co-scheduling, rescheduling, and green optimization, they are still insufficiently connected with data-driven congestion analytics and systems-oriented decision support. Second, although green shipping has received increasing attention, relatively few studies jointly consider operational efficiency, energy-related objectives, and resource constraints in a scalable multi-objective framework for a real lock hub. Third, stakeholder-oriented concerns such as fairness, resilience, and rule evaluation have only recently begun to receive attention and are not yet fully integrated into mainstream lock scheduling models. Accordingly, the present study is positioned as a bridge between these strands. It focuses on multi-objective ship lock scheduling under energy-consumption and resource constraints, and compares several Pareto-based intelligent optimization algorithms. At the same time, explicit CO_2 accounting, stronger fairness formulations, priority-based control, severe disruptions, and infrastructure power limits remain meaningful directions for future research rather than being fully modeled in the current version.

Accordingly, the revised manuscript makes the empirical logic more explicit by examining three working hypotheses.

H1. *Algorithms with a stronger many-objective search capability can reduce waiting burden while maintaining high lock utilization under the same data setting.*

H2. *An algorithm showing a more balanced trade-off across the five objectives should also display lower arrival-rescheduling pressure and lower berth-overcapacity pressure.*

H3. *As scenario scale increases, algorithmic differences become more pronounced, so no single method should be treated as uniformly dominant across all operating conditions.*

2. Problem Description and Model Establishment

2.1. Problem Description

As an important component of the regional water transport system, inland waterway locks must coordinate traffic efficiency, service reliability, energy use, and environmental pressure within a constrained operational space. Under high-demand conditions, the Da Teng Gorge Ship Lock faces concentrated vessel arrivals, limited waiting-area capacity, and dynamic disturbance factors, all of which increase the difficulty of scheduling. The schematic diagram of the Da Teng Gorge Ship Lock structure is shown in Figure 1 below. In this study, the scheduling problem is defined over a discrete decision horizon in which

arriving vessels may wait in the approach berth area and are then assigned to feasible lock service slots.

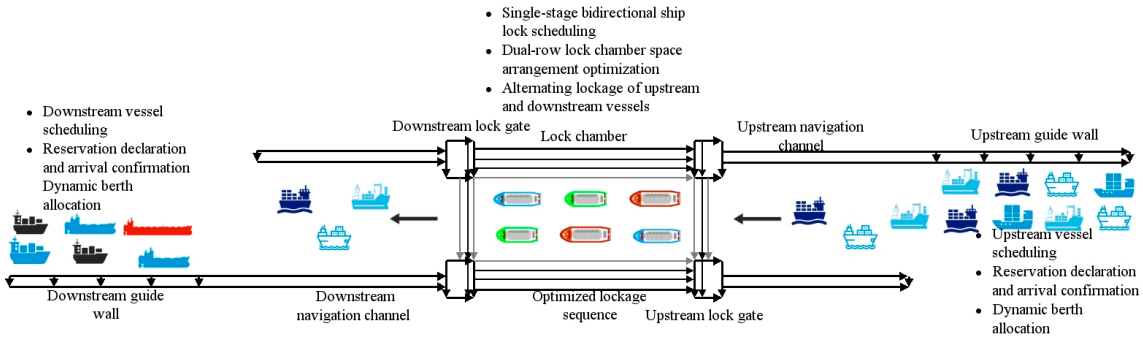


Figure 1. Structural schematic diagram of Da Teng Gorge Ship Lock.

Accordingly, the model focuses on the joint allocation of two types of resources: lock service capacity and waiting-berth capacity in the approach area. Here, the term "berth" refers to the waiting berth in the lock approach area rather than to the lock chamber itself. The berth-overcapacity penalty therefore represents the penalty incurred when the number of waiting vessels exceeds the available waiting-berth capacity. This distinction is introduced to avoid the ambiguity between lock number, berth number, and overcapacity penalty identified in the review comments.

The model is intended to generate a feasible lock scheduling plan for all vessels within the decision horizon. The optimization simultaneously considers average waiting time, lock utilization, total energy consumption, arrival rescheduling rate, and berth-overcapacity penalty, while respecting capacity, service, and operating constraints. The specific ship scheduling flowchart is shown in Figure 2 below. The purpose is not to claim a universally optimal dispatching rule, but to provide a decision-support framework that can reveal trade-offs among efficiency, energy, and resource pressure in a practically interpretable way.

The main modeling assumptions adopted in this study are as follows.

1. Dynamic demand fluctuation.

The number of vessels arriving at the lock is allowed to vary across days and time slots according to the observed arrival pattern and scenario disturbances. In this sense, the arrival process is not treated as a fixed deterministic sequence. Instead, historical variation, appointment deviation, weather-related fluctuation, and other operational disturbances are reflected through scenario-based adjustment of the arrival volume within the decision horizon.

2. Reduced-order energy-consumption representation.

The energy consumption of the lock system is affected by vessel size, traffic state, and actual service load. Because high-resolution hydrodynamic and power-measurement data are not available for every lockage cycle in the preserved dataset, this study adopts a reduced-order operational representation instead of a fully physical propulsion model. In the revised manuscript, the energy term is therefore interpreted as a condition-dependent operational estimate rather than as a universal fixed value per vessel: a baseline energy coefficient is read together with vessel-size grouping, lock-operation stage, and congestion-related service intensity. The resulting objective is suitable for comparative scheduling evaluation under consistent data conditions, although it does not attempt to replace a detailed hydrodynamic energy model.

3. Adaptive scheduling-window adjustment.

The scheduling window of the lock system is assumed to be adjustable within the slot-based decision framework. The adjustment is guided by real-time arrivals, historical patterns, queue pressure, and lock operating capacity. This assumption is used to reflect the operational possibility of moderate timing adjustment under congestion, rather than to imply unrestricted rescheduling freedom.

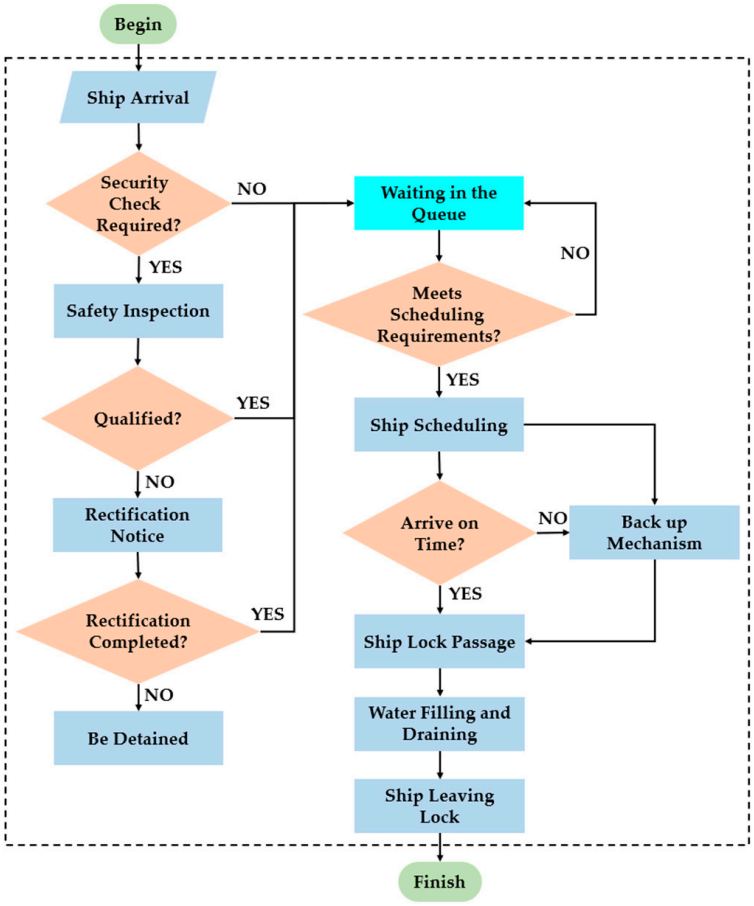


Figure 2. Flowchart of ship dispatching process at Da Teng Gorge Ship Lock.

2.2. Model Parameters

Definitions of parameters and variables.

For clarity, the key parameters and decision variables are summarized in Table 1. In the revised manuscript, the average waiting time is defined over all vessels within the decision horizon rather than over cargo tonnage; the lock-capacity parameters describe the number of vessels that can be processed by the chamber in one scheduling slot; and the berth-capacity parameters refer to the waiting-berth capacity in the approach area. This clarification is intended to strengthen the physical interpretation of the model and reduce ambiguity in the notation.

To avoid notation-related misunderstanding, the index system is further clarified here. N denotes the number of days in the decision horizon, and I denotes the number of discrete scheduling periods within one day. Therefore, the pair (n, i) represents time period i on day n, rather than the total number of ships over N × I. Similarly, the average waiting time of all ships means the mean waiting burden of all vessels included in the decision horizon, whereas the adjusted-arrival variable denotes the number of vessels remaining in or reassigned to a given period after rescheduling and carry-over effects are considered.

Table 1. Definitions of parameters and variables for the ship lock scheduling model.

Symbols	
f_1	Average waiting burden of all vessels within the decision horizon
f_2	Ratio of actual serviced vessels to slot-level lock service capacity
f_3	Total operational energy associated with vessel service and lock passage over the decision period
f_4	Proportion of vessels whose actual service period deviates from the original arrival or appointment period
f_5	Penalty incurred when waiting demand exceeds the available approach-berth capacity
N	Number of days in the decision horizon
I	Number of discrete scheduling periods into which one day is divided
Q_{ni}	Adjusted number of arriving vessels in period i on day n after rescheduling
A_{ni}	Initially observed number of arrivals in period i on day n before rescheduling
B_{ni}	Carry-over demand from the previous period or previous day that remains to be serviced
μ_{ni}	Service capacity of period i on day n, measured by the number of vessels that can be processed
ρ_{ni}	Scheduling weight assigned to period i on day n
l_{max}	Maximum number of vessels that can be processed by the lock in one scheduling period
r_e	Baseline energy-consumption coefficient per vessel under the adopted reduced-order operational model
C_{berth}	Maximum number of vessels that can wait in the approach-berth area
P_{over}	Penalty coefficient applied when waiting demand exceeds berth capacity
σ_B	Variance of berth utilization across periods, reflecting the balance of berth use
P_B	Fairness-penalty function used to discourage concentrated use of only a small subset of berths
$y_{ni} \in R^+$	Decision variable representing the number of vessels scheduled for service in period i on day n

2.3. Proposed Ship Lock Scheduling Model

Efficient ship lock scheduling should improve lock service efficiency while maintaining an interpretable balance among time, energy, and waiting-area resource pressure. For this reason, the model is formulated as a coordinated multi-objective scheduling problem rather than as a purely throughput-oriented dispatching rule. The revised manuscript places greater emphasis on the operational meaning of each objective and on the distinction between measured quantities, management targets, and scenario-based parameters.

The model plans the time and resource allocation of vessels passing through the lock through mathematical optimization. Its objective is to support decision making under practical constraints rather than to reproduce every physical detail of lock operation. Accordingly, the formulation is designed to jointly consider waiting burden, lock utilization, energy expenditure, arrival adjustment, and berth-overcapacity pressure, while keeping the optimization structure sufficiently clear for algorithmic comparison and managerial interpretation.

The proposed model is described as follows.

Objective:

To preserve consistency with Pareto-based evolutionary algorithms, the five objective functions are retained as a genuine multi-objective formulation during optimization. If managerial preference analysis is required, weighting factors may be introduced only after the non-dominated solution set has been generated, so that candidate schedules can be ranked under specific policy preferences without collapsing the optimization problem into a single-objective surrogate at the search stage.

$$minF = \omega_1 f_1 + \omega_2(-f_2) + \omega_3 f_3 + \omega_4 f_4 + \omega_5 f_5 \tag{1}$$

The first objective represents the average waiting time of all vessels within the decision horizon.

$$f_1 = \frac{1}{NI} \sum_{n=1}^{N} \sum_{i=1}^{I} \frac{Q_{ni}}{\mu_{ni} \rho_{ni}} \tag{2}$$

The second objective represents lock utilization and reflects the efficiency of service-capacity use.

$$f_2 = \frac{1}{Nl \ \ max\sum_{n=1}^{N}\sum_{i=1}^{I} Q_{ni}} \tag{3}$$

The third objective represents the total energy consumption associated with lock service and vessel passage under the adopted operational energy model.

$$minf_3 = \sum_{n=1}^{N}\sum_{i=1}^{I} Q_{ni}{\cdot}r_e \tag{4}$$

The fourth objective represents the arrival rescheduling rate and describes the deviation between the observed arrival sequence and the implemented service schedule.

$$minf_4 = \frac{1}{NI}\sum_{n=1}^{N}\sum_{i=1}^{I}\frac{|A_{ni} - Q_{ni}|}{A_{ni}} \tag{5}$$

The fifth objective represents the berth-overcapacity penalty, that is, the penalty incurred when the number of waiting vessels exceeds the available waiting-berth capacity. In addition, carbon impact is reported as a derived indicator linked to total energy consumption, rather than as a duplicated objective with exactly the same optimization direction.

For reproducibility, Equations (1)–(5) are interpreted as the measures of queueing burden, service-capacity use, operational energy expenditure, schedule-deviation pressure, and waiting-area overcapacity, respectively. Equations (7)–(21) then define the feasible operating region through non-negativity, lock-capacity, berth-capacity, waiting-time benchmark, daily-throughput requirement, energy benchmark, berth-balance monitoring, no-show tolerance, arrival-rescheduling control, and dispatch-continuity conditions. These additions are intended to make the mathematical formulation easier to read, implement, and verify.

$$minf_5 = \sum_{n=1}^{N} max(0, \sum_{i=1}^{I} Q_{ni} - C_{berth}){\cdot}P_{over} \tag{6}$$

Constraints:

The number of ships passing through locks should be non-negative.

$$Q_{ni} \geq 0, \quad \forall i \in I, \forall n \in N \tag{7}$$

The operational efficiency of the locks is between 0 and 1.

$$0 \leq \mu_{ni} \leq 1 \tag{8}$$

The parameters related to the ship must be non-negative and consistent.

$$p_{ni} \geq 0 \tag{9}$$

The number of ships scheduled must not exceed the maximum berth capacity of the lock.

$$\sum_{i=1}^{l} Q_{ni} \leq C_{barth}, \ \forall n \tag{10}$$

The number of ships passing through the lock must not exceed its maximum capacity during each scheduling cycle.

$$\sum_{n=1}^{N} Q_{ni} \leq l_{max} \tag{11}$$

A 48 h upper waiting-time target is introduced as a managerial benchmark for scenario evaluation rather than as a universal physical constant.

$$\frac{1}{NI}\sum_{n=1}^{N}\sum_{i=1}^{I}\frac{Q_{ni}}{\mu_{ni}\rho_{ni}} \leq 48 \tag{12}$$

A minimum daily service volume of 42 vessels is adopted according to the observed operating requirement in the study period.

$$\sum_{n=1}^{\infty} Q_{ni} \geq 42, \ \forall i \tag{13}$$

The 65,000 kWh daily energy ceiling is treated as an operational benchmark used for dispatch evaluation and sensitivity analysis.

$$\sum_{n=1}^{N}\sum_{i=1}^{l} Q_{ni} \cdot r_e \leq 65,000 \tag{14}$$

The variance in berth utilization is monitored in order to reflect the fairness of waiting-berth usage across the scheduling horizon.

$$\sigma_B = \sqrt{\frac{1}{N}\sum_{n=1}^{N}(\sum_{i=1}^{I} Q_{ni} - \frac{1}{N}\sum_{n\prime=1}^{N}\sum_{i=1}^{I} Q_{n\prime i})^2} \tag{15}$$

The berth-fairness penalty is calculated to discourage persistent concentration of waiting vessels in only a small subset of available berths.

$$P_B = 20\sigma_B \tag{16}$$

A reservation no-show rate of 20% is used as an upper scenario bound rather than as a universal empirical constant.

$$\frac{1}{NI}\sum_{n=1}^{N}\sum_{i=1}^{I}\frac{|A_{ni} - Q_{ni}|}{A_{ni}} \leq 0.2 \tag{17}$$

The arrival-rescheduling rate is constrained to limit excessive deviation between appointments and actual service order.

$$\frac{1}{NI}\sum_{n=1}^{N}\sum_{i=1}^{I}\frac{|A_{ni} - Q_{ni}|}{A_{ni}} \leq 0.3 \tag{18}$$

The number of dispatches in each time period must be at least one.

$$y_{ni} \geq 1, \ \forall n, i \tag{19}$$

The threshold values in Equations (12)–(20) are not treated as immutable physical laws. In the revised manuscript, they are interpreted as a combination of historical operating observations, management benchmarks, and scenario settings used for the robustness evaluation.

$$|y_{n+1,i} - y_{ni}| \leq 10, \ \forall n, i \tag{20}$$

$$Q_{ni} = \begin{cases} y_{ni}, & if \ A_{ni} - B_{ni} \geq y_{ni} \\ A_{ni} - B_{ni} + y_{ni}, & otherwise \end{cases} \tag{21}$$

3. Algorithm Design

3.1. Algorithmic Analysis

The ship lock scheduling problem involves multiple conflicting optimization objectives, such as minimizing the average waiting time, maximizing the lock utilization rate, minimizing the total energy consumption, minimizing the arrival repositioning rate, and minimizing the penalty for exceeding the mooring capacity. Therefore, it is crucial to use an efficient multi-objective optimization algorithm to find the optimal scheduling solution under complex constraints. In this study, four advanced multi-objective optimization algorithms, namely NSGA-II, NSGA-III, SPEA-II and MOEA/D, are selected and their optimization performance is analyzed in depth. Among them, NSGA-II is a classical multi-objective evolutionary algorithm that has been widely used in complex scheduling optimization problems due to its superior computational efficiency and stable convergence of the Pareto solution set. Its core idea is to guide the search based on non-dominated sorting and congestion distance, so as to improve both the quality and the uniformity of the solution. NSGA-III shows stronger performance in dealing with high-dimensional objective optimization problems, and has achieved remarkable results in practical applications such as ship scheduling and stowage optimization. In addition, MOEA/D, as a decomposition-based multi-objective evolutionary algorithm, shows good convergence and solution diversity by decomposing multi-objective problems into several subproblems and solving them in parallel. It is suitable for complex scheduling optimization scenarios [29,30].

3.2. Algorithm Experiment Steps

The NSGA-II algorithm is used as an example to illustrate the implementation of the algorithm steps, as shown in Figure 3. This algorithm uses a genetic evolutionary mechanism to continuously optimize the scheduling plan during the search process, ensuring that the final solution set can effectively balance different optimization objectives and provide an efficient and feasible optimization strategy for ship scheduling [31].

3.2.1. Genetic Algorithm Implementation Steps

Step 1: The scheduling problem is first encoded on the basis of lock assignment, waiting-berth allocation, and service sequence. The initialization stage specifies the key operating parameters, including the decision horizon, the number of daily scheduling slots, lock capacity, waiting-berth capacity, vessel arrival information, and time-related service data. In the revised implementation, the encoding is designed to remain feasible with respect to lock-capacity and waiting-area constraints as far as possible before evolutionary variation is applied.

1. Arrival Berth Scheduling Code: defines vector $C^{(1)} = \{b_1, b_2, \ldots, b_n\}$, where $b_j \in \{1, 2, \ldots, B\}$ denotes the berth to which vessel j is assigned.
2. Lock Scheduling Encoding: define vector $C^{(2)} = \{l_1, l_2, \ldots, l_n\}$, where $l_j \in \{1, 2, \ldots, L\}$ denotes the lock number to which the ship j is assigned.

3. Lock Passing Sequence scheduling encoding: use a vector with a length of n alignment vector $C^{(3)} = \pi\{v_1, v_2, \ldots, v_n\}$ 1 is used to represent the ship's lock-passing sequence.

The final chromosome can be represented as a three-dimensional coding string.

$$C_j = \left(C^{(1)}, C^{(2)}, C^{(3)}\right) \in Z^{3\times n} \tag{22}$$

Step 2: After the encoding structure is determined, the initial population is generated. Each individual represents a candidate scheduling scheme. During initialization, feasibility checks are applied to reduce obvious violations of berth assignment, lock-capacity limits, and service timing. Heuristic perturbation rules based on berth load and vessel-arrival distribution are used to improve diversity while keeping the initial solutions operationally interpretable.

Step 3: In each generation, a non-dominated ordering is performed on the current population P_t to partition the set of non-dominated frontier solutions Z_t. Based on the Pareto dominance relation:

$$\forall C_i, C_j \in P_t, C_i < C_j \Leftrightarrow \exists f_k(C_i) < f_k\left(C_j\right) \wedge \forall m, f_m(C_i) \leq f_m\left(C_j\right) \tag{23}$$

For the individuals in Z_t their five objective function values $F\left(C_j\right)$ are obtained and combined with Crowding Distance to calculate the fitness, which reflects the dominance advantage and diversity distribution of individuals in the target space.

Step 4: The non-dominated set Z_t are moved_into the next generation of the parent population P_{t+1}. If P_{t+1} then the crowding degree distance ranking mechanism retains the most diverse individuals making $|P_{t+1}| = \mathrm{N}$:

$$CrowdingDistance(i) = \sum_{k=1}^{M} \frac{f_k^{(i+1)} - f_k^{(i-1)}}{f_k^{max} - f_k^{min}} \tag{24}$$

Step 5: Paired individuals are selected from the parent population and subjected to crossover. The operators are applied to berth allocation, lock assignment, and service sequence in a coordinated manner so that exploration is improved without destroying the logical relationship among the three coding segments.

Step 6: Genetic variation (including berth, order & lock assignment variation) is applied to the offspring population with probability P_m to enhance the global search capability and prevent from falling into a local optimum.

Step 7: The offspring population Q_{t+1}, generated through crossover and mutation, together with the current parent P_{t+1}, constitutes the candidate population $R_{t+1} = P_{t+1} \cup Q_{t+1}$. The iteration continues by constructing a new elite population P_{t+1} replacing the previous generation through non-dominated sorting and crowding assessment.

Step 8: The algorithm terminates when the maximum number of generations is reached or when the Pareto front becomes sufficiently stable. In the revised framework, robustness is not treated only as an ex post deletion rule. Instead, candidate schedules are additionally evaluated under moderate arrival perturbation, no-show, and temporary capacity-loss scenarios, and the resulting violation penalty is fed back into environmental selection. This setting makes the robustness treatment more consistent with the evolutionary search process.

$$TotalCost = \sum_{j=1}^{n} \left(c_{wait} w_j + c_{lock} u_j + c_{energy} e_j\right) \tag{25}$$

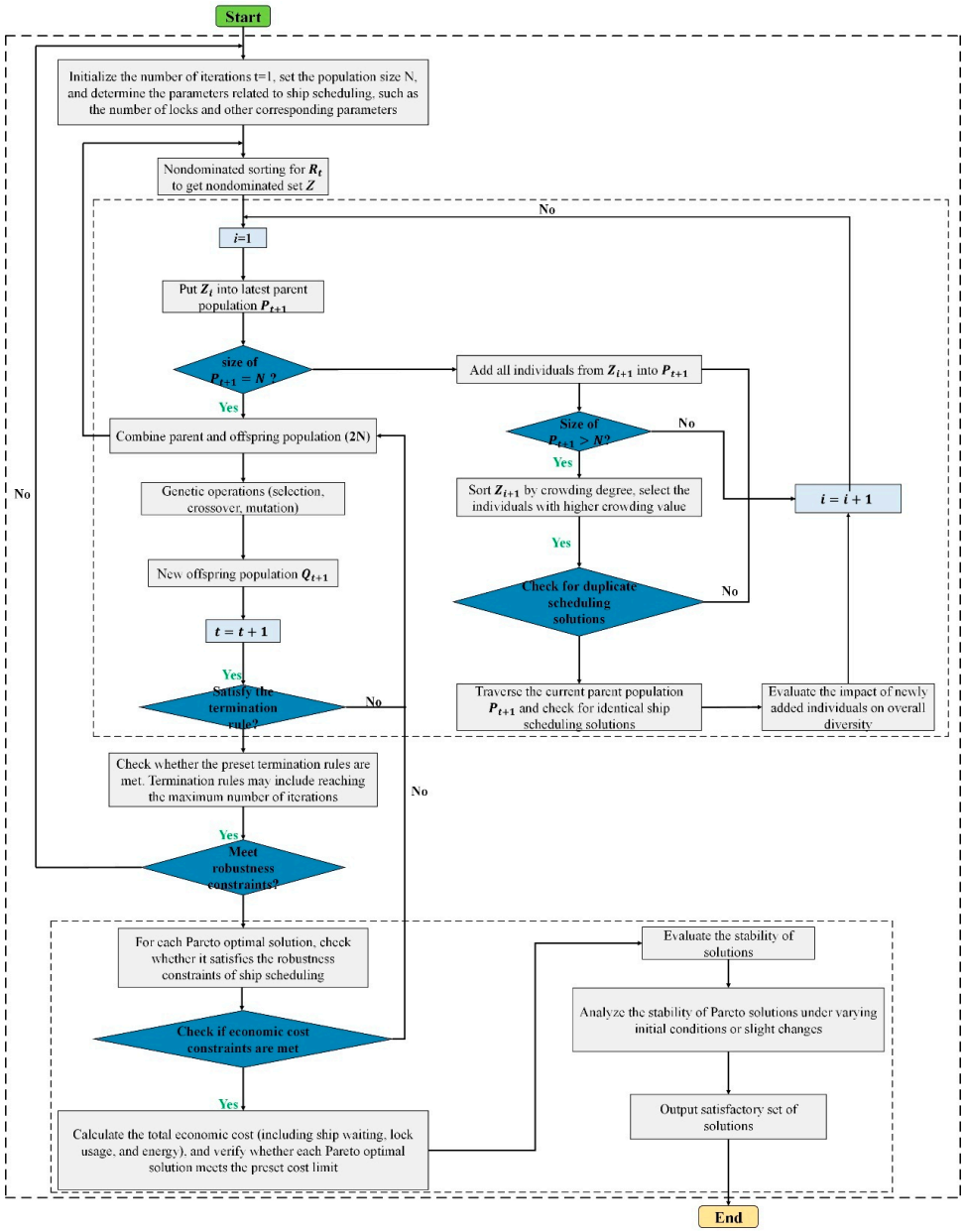


Figure 3. Algorithm experimentation steps.

3.2.2. Vessel Coding Scheme

1. Arrival Berth Dispatch Code

It is represented as a four-row coding matrix:

$$C^{(1)} = \begin{bmatrix} b_1 & b_2 & \cdots & b_n \\ a_1 & a_2 & \cdots & a_n \\ d_1 & d_2 & \cdots & d_n \\ p_1^{berth} & p_2^{berth} & \cdots & p_n^{berth} \end{bmatrix} \in Z^{4\times n} \quad (26)$$

Row 1 (berth number): the first j berth to which the vessel is assigned $b_j \in \{1, 2, \ldots, B\}$.

Row 2 (time of arrival): a_j Indicates the time the vessel arrived at the berth area.

Row 3 (time of departure from berth): d_j indicates the expected time of departure from the berth and can be used to calculate the berth occupancy cycle.

Row 4 (Berth Priority): P_j^{berth} indicates the ship's preference/weight for the berth, which is used for berth optimization scheduling (e.g., shortest berth waits).

2. Lock Dispatch Code

It is represented as a four-row coding matrix:

$$C^{(2)} = \begin{bmatrix} l_1 & l_2 & \cdots & l_n \\ t_1^{est} & t_2^{est} & \cdots & t_n^{est} \\ s_1 & s_2 & \cdots & s_n \\ p_1^{lock} & p_2^{lock} & \cdots & p_n^{lock} \end{bmatrix} \in Z^{4\times n} \quad (27)$$

Row 1 (berth number): the first j berth to which the ship is assigned $b_j \in \{1, 2, \ldots, B\}$.

Row 2 (time of arrival): a_j indicates the time the vessel arrived at the berthing area.

Row 3 (time of departure from berth): d_j indicates the expected time of departure from the berth and can be used to calculate the berth occupancy cycle.

Row 4 (Berth Priority) P_j^{berth} indicates the ship's preference/weight for the berth, which is used for berth optimization scheduling (e.g., shortest berth waits).

3. Lock Passing Sequence

It is represented as a four-row coding matrix:

$$C^{(3)} = \begin{bmatrix} v_1 & v_2 & \cdots & v_n \\ \tau_1 & \tau_2 & \cdots & \tau_n \\ g_1 & g_2 & \cdots & g_n \\ \phi_1 & \phi_2 & \cdots & \phi_n \end{bmatrix} \in Z^{4\times n} \quad (28)$$

Row 1 (crossing order): the ship number of the crossing queue v_j, is the length of the n of the full alignment.

Row 2 (time taken to pass through the lock): τ_j indicates the time the vessel is expected to take to pass through the lock.

Row 3 (group number): g_j indicates the crossing scheduling group in which the vessel is located for batch control or formation scheduling.

Row 4 (Priority Passage Flag): $\varnothing_j \in \{0, 1\}$, with 1 indicating that it is a Privileged/Emergency Passage Vessel, which can be prioritized.

3.2.3. Example Explanation of the Scheduling Program

1. Arrival Berth Dispatch Code

Arrival berth scheduling scheme coding example analysis shown in Figure 4, the data structure contains four rows of content: the first act of the ship assigned berth number b_j (such as the terminal has three berths); the second act of the arrival berth time a_j, said the ship actually arrived at the berth area of the time; third act of the time to leave the berth d_j, that is, expected to leave the berths of the time, reflecting the use of berths cycle. The 4th line is the berth priority P_j^{berth}, which indicates the degree of preference for the berth, and can be used to optimize the berth scheduling or the associated waiting time penalty mechanism.

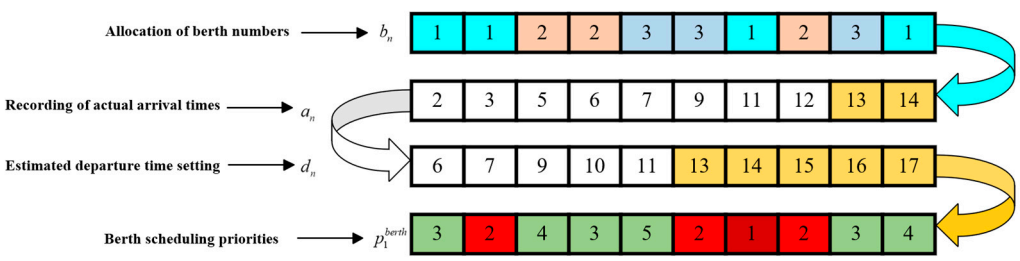


Figure 4. Gantt chart of arrival berth scheduling codes.

2. Lock Dispatch Code

An example analysis of the coding of the lock scheduling scheme is shown in Figure 5. The data structure contains four rows of information: row 1 is the lock number assigned to the ship (e.g., 1 for the upper gate of Daito Gorge, 2 for the lower gate); row 2 is the estimated time of lock entry t_j^{est}, which indicates the time when the ship is scheduled to arrive and request to enter the lock; row 3 is the size of the ship s_j, categorized by tonnage class (1 = small, 2 = medium, 3 = large), which is used to limit the capacity of the lock; and row 4, Lock Priority P_j^{lock}, which is used to determine the queuing priority of the vessel in the scheduling, and also serves as the basis for the penalty mechanism.

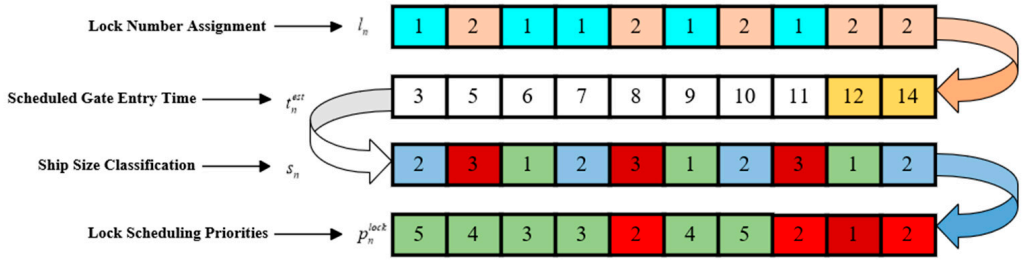


Figure 5. Gantt chart of scheduling codes to the locks.

3. Lock Passing Sequence

Arrival berth scheduling scheme coding example analysis shown in Figure 6, the data structure includes four items: the first act of the order of crossing the gate v_j, indicating that the ship passes through the successive arrangement (1~10 of the arrangement); the second act of the passage of the gate time-consuming τ_j, that is, the time required for each ship to pass through the locks; third act of the passage of the gate grouping g_j, for the identification of the ship's scheduling group (such as each group) three ships pass through the lock together); and the 4th row is the priority $\varnothing_j$, which is a 0/1 flag, where 1 means that the ship is a priority or emergency ship and will be given priority in the queue.

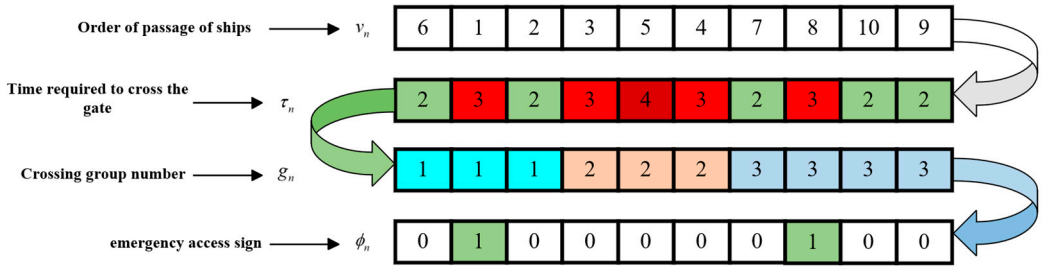


Figure 6. The crossing sequence scheduling coding Gantt chart.

As shown in Figure 7, spatial layout and time control mechanism of port ship scheduling is systematically displayed, covering key operational areas such as Lock 1, Lock 2, Waiting Area, Entry Area and Anchorage Area. Different ships are distributed in each functional area according to their numbers, and the expected gate entry time and planned berthing time of each ship are clearly labeled in Entry Area and Anchorage Area. This kind of layout not only reflects the efficient use of space resources by the port scheduling system, but also emphasizes the precise management of time dimension. Through the orderly arrangement of ships in each functional area and the dynamic coordination of time nodes, it can effectively improve port operation efficiency, reduce the waiting time of ships in port, and optimize the operation rhythm and logistics smoothness of the whole shipping chain.

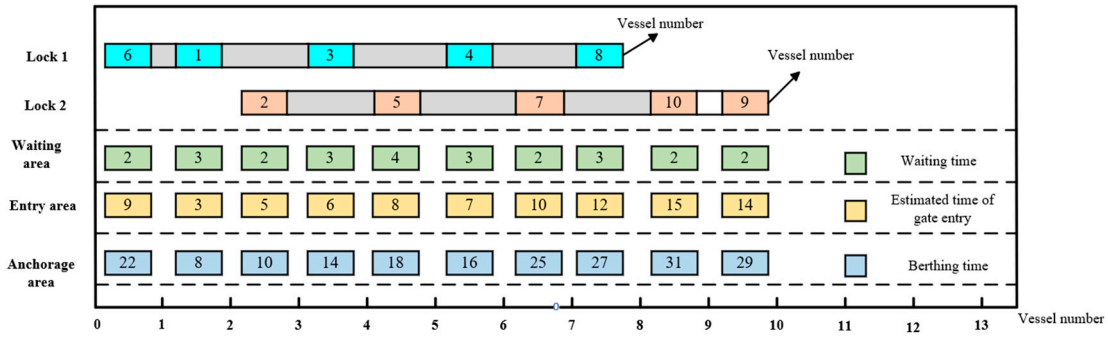


Figure 7. Layout map of port ship scheduling with multi-region collaboration and visualization of its time control mechanism.

4. Experiment and Result Analysis

4.1. Data Source

The empirical analysis is based on field data collected for vessels passing through the Da Teng Gorge Ship Lock Hub from 9 May to 23 May 2024. To improve comparability, the preserved records are reorganized into a one-week decision horizon, yielding an empirical instance with 594 vessels. In accordance with the observed operating rhythm of the lock, each day is divided into 16 appointment slots. Table 2 reports the observed arrival pattern, and Table 3 reports the main parameter settings. In the revised manuscript, these parameter values are interpreted more explicitly: some are measured or directly estimated from operations, whereas others are managerial benchmarks or scenario settings introduced for robustness analysis.

Table 2. Data on the arrival of ships at various times during the decision period.

Appointment Time i	Arrival Time	Number of Ships Arriving A_{ni}			
		$N = 1$	$N = 2$	$N = n$	$N = 7$
1	0:00–2:00	2	2	…	7
2	2:00–4:00	4	5	…	5
3	4:00–6:00	5	4	…	6
4	6:00–8:00	3	6	…	3
5	8:00–9:00	6	3	…	5
6	9:00–10:00	4	5	…	4
7	10:00–11:00	5	4	…	3
8	11:00–12:00	3	6	…	5
9	12:00–13:00	6	3	…	4
10	13:00–14:00	4	5	…	6
11	14:00–15:00	5	4	…	3
12	15:00–16:00	3	6	…	5
13	16:00–17:00	6	3	…	4
14	17:00–18:00	4	5	…	6
15	18:00–20:00	5	4	…	3
16	20:00–24:00	3	6	…	5

Among the parameters reported in Table 3, the energy-related coefficient should be understood as a baseline coefficient under a reference operating state. In the computational interpretation, its effect is considered together with vessel-size grouping, lock-cycle load, and disturbance-related service intensity so that the environmental objective remains responsive to operating conditions instead of being read as a completely static constant.

Table 3. Parameter settings for problem instance generation.

Notation	Parameters Used to Generate Problem Instances	
	Parameter Meaning	**Parameter Value**
N	decision period coefficient	7
I	daily appointment time slot	16
A	number of ships arriving	594
μ	service rate	[6,9]
a, b	adjustment time window allocation coefficients	2.0, 5.0
l_{max}	maximum gate throughput	12
S_{max}	maximum length of the ship lock	280
e	maximum service volume per time slot	4
O	queue threshold	8
α	penalty coefficient	0.85
E_r	baseline energy-consumption coefficient under reference operating state	3.2
N_{sr}	no-show rate	0.05
β	penalty coefficient for rescheduling of arrivals	200
B_c	berth capacity	10
αCO_2	carbon emission coefficient	2.587
g	berth penalty coefficient	0.2
p_{oc}	over-berth capacity penalty	800
r_t	recovery time after equipment failure	2.0
h_w	historical arrival pattern coefficient of ships	0.7
p_{et}	real-time prediction error tolerance	0.2

4.2. Green Ship Scheduling Optimization Based on Multi-Objective Optimization Algorithms and System Robustness Analysis

This section evaluates green ship scheduling and system robustness under the proposed multi-objective framework. Four representative algorithms—NSGA-II, NSGA-III, SPEA-II, and MOEA/D—are implemented in Python 3.10.10 and compared with respect to five operational indicators: average waiting time, lock utilization, total energy consumption, arrival rescheduling rate, and berth-overcapacity penalty. The parameter settings for the four algorithms are shown in Table 4 below. The emphasis of the revised analysis is placed on trade-off behavior, robustness, and practical interpretability, rather than on isolated best-value claims unsupported by a complete set of repeated-run statistics.

Table 4. Four algorithm parameter settings tables.

Algorithm	Population	Generations	Crossover	Mutation	Special Settings
NSGA-II	100	200	0.90	0.10	Tournament size = 2; elitist non-dominated sorting
NSGA-III	100	200	0.90	0.10	Reference points generated for five objectives
SPEA-II	100	200	0.90	0.10	Archive size = 100
MOEA/D	100	200	0.90	0.10	Neighborhood size = 20; decomposition weights generated uniformly

To improve the traceability between the study propositions and the empirical evidence, the revised results section is interpreted against H1–H3. All four algorithms are evaluated under the same decision horizon, arrival dataset, population size, generation limit, crossover probability, and mutation probability so that the comparison focuses on search behavior rather than on inconsistent computational budgets. At the same time, because the fully archived repeated-run records and formal parameter-sensitivity logs for the preserved

empirical instance are incomplete, the revised manuscript avoids statistical-significance claims and reports the findings as case-based comparative evidence.

As shown in Figures 8 and 9, a comparative analysis is conducted for the 594-vessel empirical instance from the perspective of five key objectives: average waiting time, lock utilization, total energy consumption, arrival rescheduling rate, and berth-overcapacity penalty. The preserved results suggest that NSGA-III and MOEA/D exhibit stronger overall trade-off behavior across most objective dimensions. Among them, NSGA-III shows the most balanced performance in terms of waiting control, energy use, and overcapacity management, indicating stronger adaptability in a multi-objective conflict environment. This conclusion, however, is interpreted cautiously and refers to the preserved empirical instance rather than to a universal ranking across all possible scheduling settings.

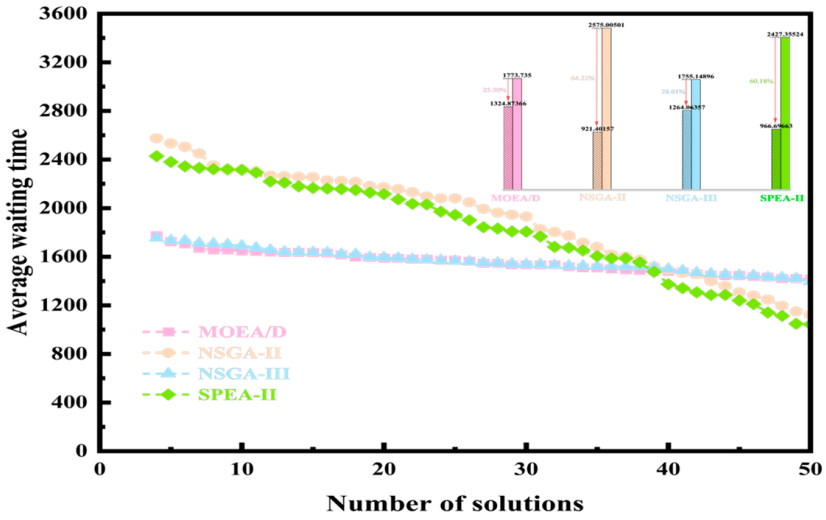


Figure 8. The evolutionary trend of the average waiting time over the number of iterations for the different multi-objective optimization algorithms.

With respect to H1, NSGA-III and MOEA/D converge to average-waiting-time values of 1530.55 and 1533.94, respectively. In the preserved empirical instance, both values are lower than those recorded for NSGA-II and SPEA-II, indicating better queue-control capability under the same data setting. To avoid ambiguity, the revised manuscript no longer uses percentage reductions unless the comparator is explicitly identified and numerically available in the archived records. Because the preserved empirical comparison is based on representative-run records rather than on a complete repeated-run archive, confidence intervals are not reported and the discussion is restricted to case-based comparative evidence.

With respect to H2, NSGA-III and MOEA/D also show comparatively stable robustness-related performance. Their arrival-rescheduling rates are 0.08281 and 0.07119, respectively, both lower than those recorded for NSGA-II and SPEA-II in the same preserved setting. The berth-overcapacity penalty follows the same directional pattern, suggesting that algorithms with a more balanced multi-objective trade-off also alleviate waiting-area pressure more effectively. For the same reason, vague statements such as 'lower than other algorithms' have been replaced by explicit algorithm names wherever the archived values allow a direct comparison.

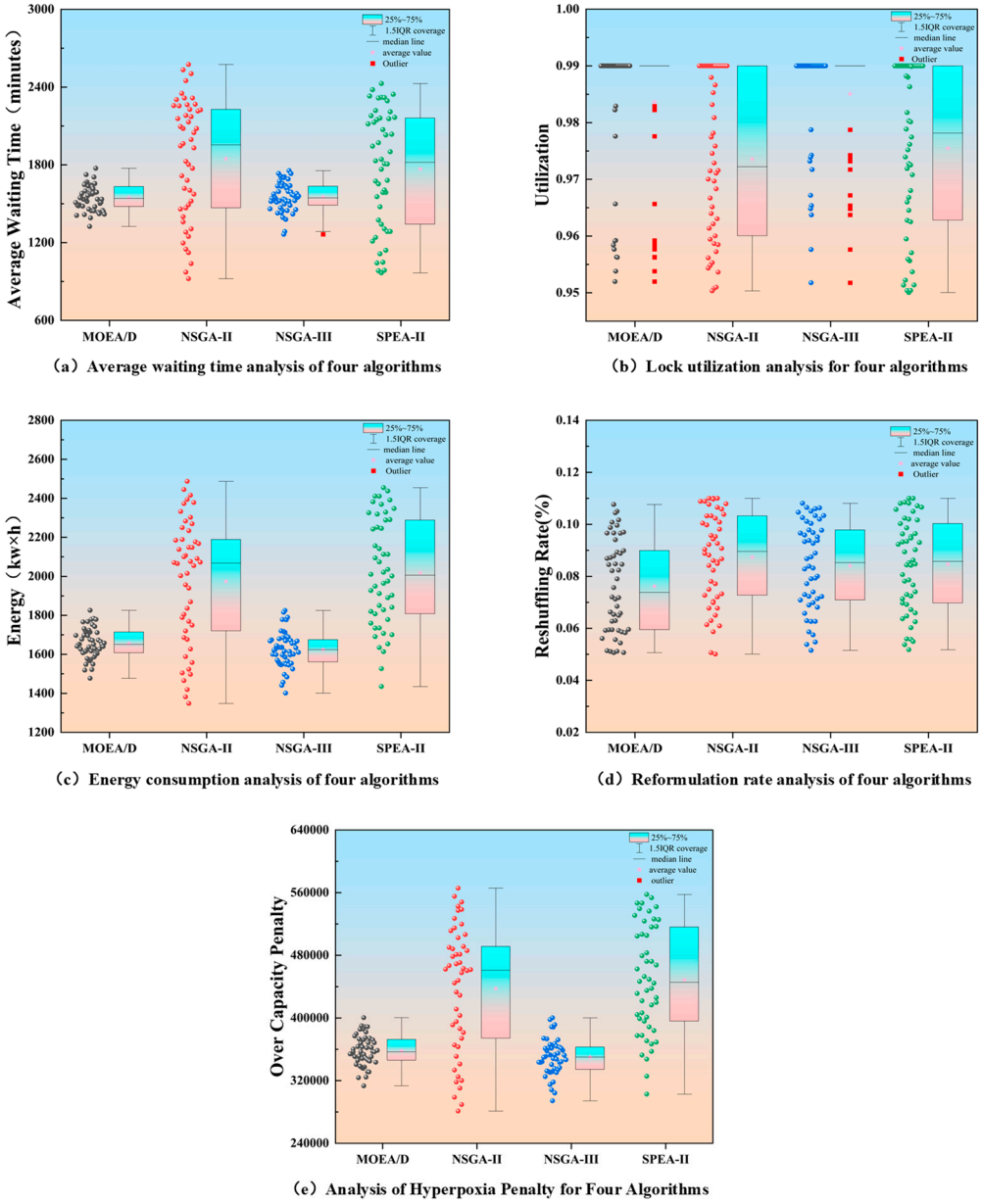


Figure 9. Experimental comparison of four multi-objective optimization algorithms in ship scheduling—based on the analysis of five key optimization objectives.

4.3. Performance Evaluation and Strategy Selection of Multi-Objective Optimization Algorithms in Ultra-Large-Scale Ship Scheduling

With respect to H3, the ultra-large-scale scenarios further show that algorithmic differences become more visible as problem size increases. The preserved results suggest that NSGA-III remains the most balanced algorithm in terms of overall trade-off quality, while MOEA/D is more competitive in strongly time-sensitive cases. SPEA-II can obtain short waiting times in some extreme scenarios, but this may be accompanied by higher energy use. By contrast, NSGA-II becomes less stable as the scenario scale increases, which indicates a potential scalability limitation rather than an across-the-board inferiority claim.

To enhance the interpretability of algorithm applicability, this paper further summarizes the preserved analysis of large-scale stress-test scenarios involving 500–1000 vessels. These scenarios are intended as offline planning-oriented stress tests rather than as direct one-to-one representations of routine daily operation at the Da Teng Gorge Ship Lock Hub. As shown in Figure 10, NSGA-III exhibits the best overall balance, with median

energy consumption of 1614.39–1643.52 kWh, a rescheduling-rate range of 7.43–9.62%, and a high proportion of non-dominated solutions with lock utilization close to 0.99. MOEA/D retains a clear advantage in waiting-time-sensitive contexts, while SPEA-II can still generate low-waiting solutions in some bursty scenarios at the cost of greater energy burden.

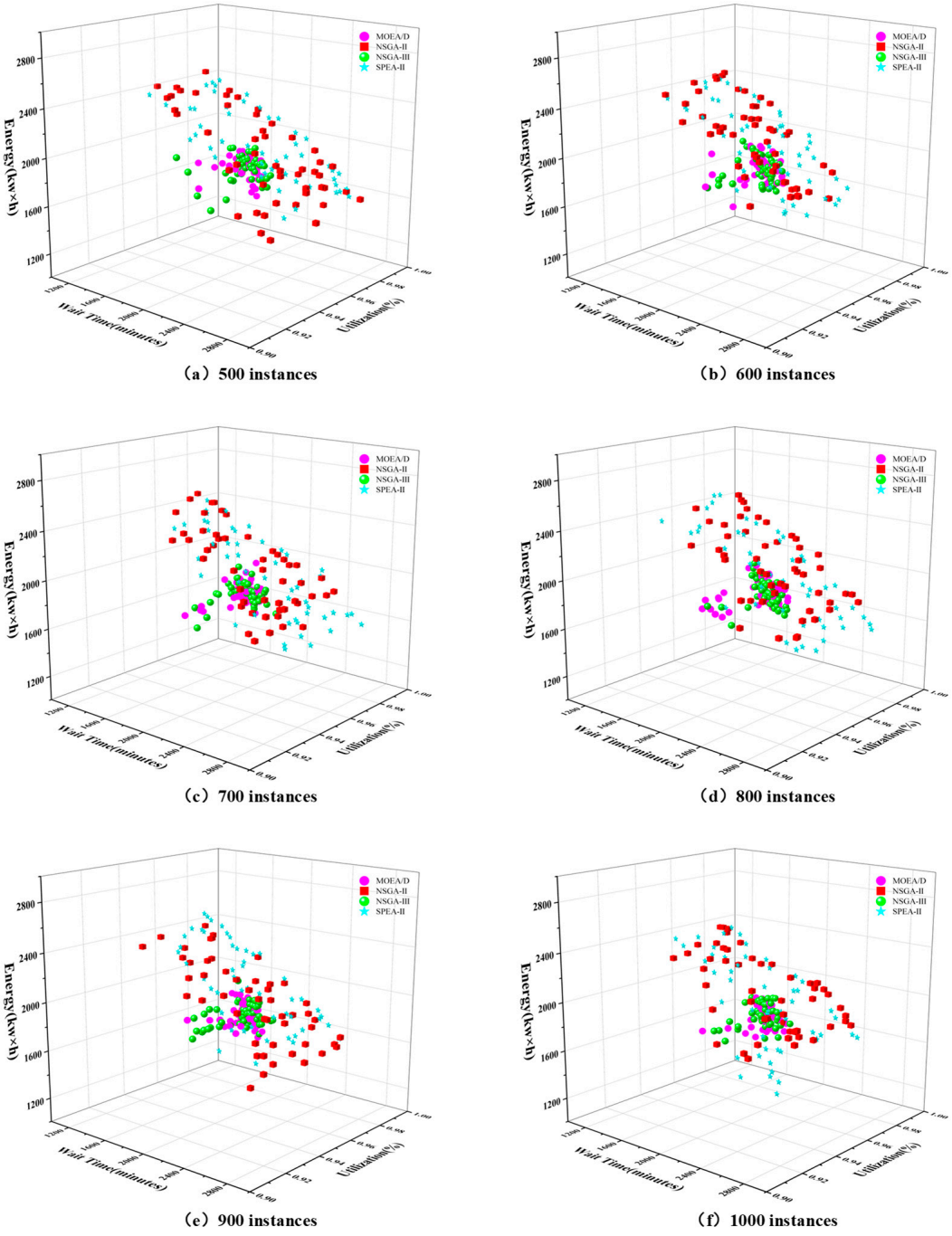


Figure 10. 3D solution set based on the six instances collected under the four algorithm conditions.

Further analysis indicates that significant nonlinear conflicts exist among the scheduling objectives, and that algorithm performance tends to diverge more clearly under ultra-large-scale conditions. Within the preserved solution set, NSGA-III achieves a comparatively good balance between hypervolume (HV = 0.873–0.892) and convergence accuracy (ε = 0.078–0.092), while MOEA/D improves temporal response through decomposition and SPEA-II retains value in some burst-task scenarios because of its archive-maintenance mechanism. These results are interpreted as comparative evidence within a common com-

putational setting, not as formally significant superiority claims across all possible runs and parameter combinations.

Overall, the preserved large-scale analysis suggests that NSGA-III provides the best balance between convergence, diversity, and system-level stability under complex constraints, whereas MOEA/D is a useful option for highly time-sensitive transportation tasks. SPEA-II retains practical value in specific extreme-response scenarios, and NSGA-II would require further strengthening if it is to remain competitive under very high load. Future work should therefore focus on adaptive reference-point evolution, dynamic switching among algorithms, and stronger integration of online operational information.

4.4. Performance Evaluation and Scalability Analysis of Multi-Objective Optimization Algorithms for Complex Inland Waterway Scheduling Scenarios

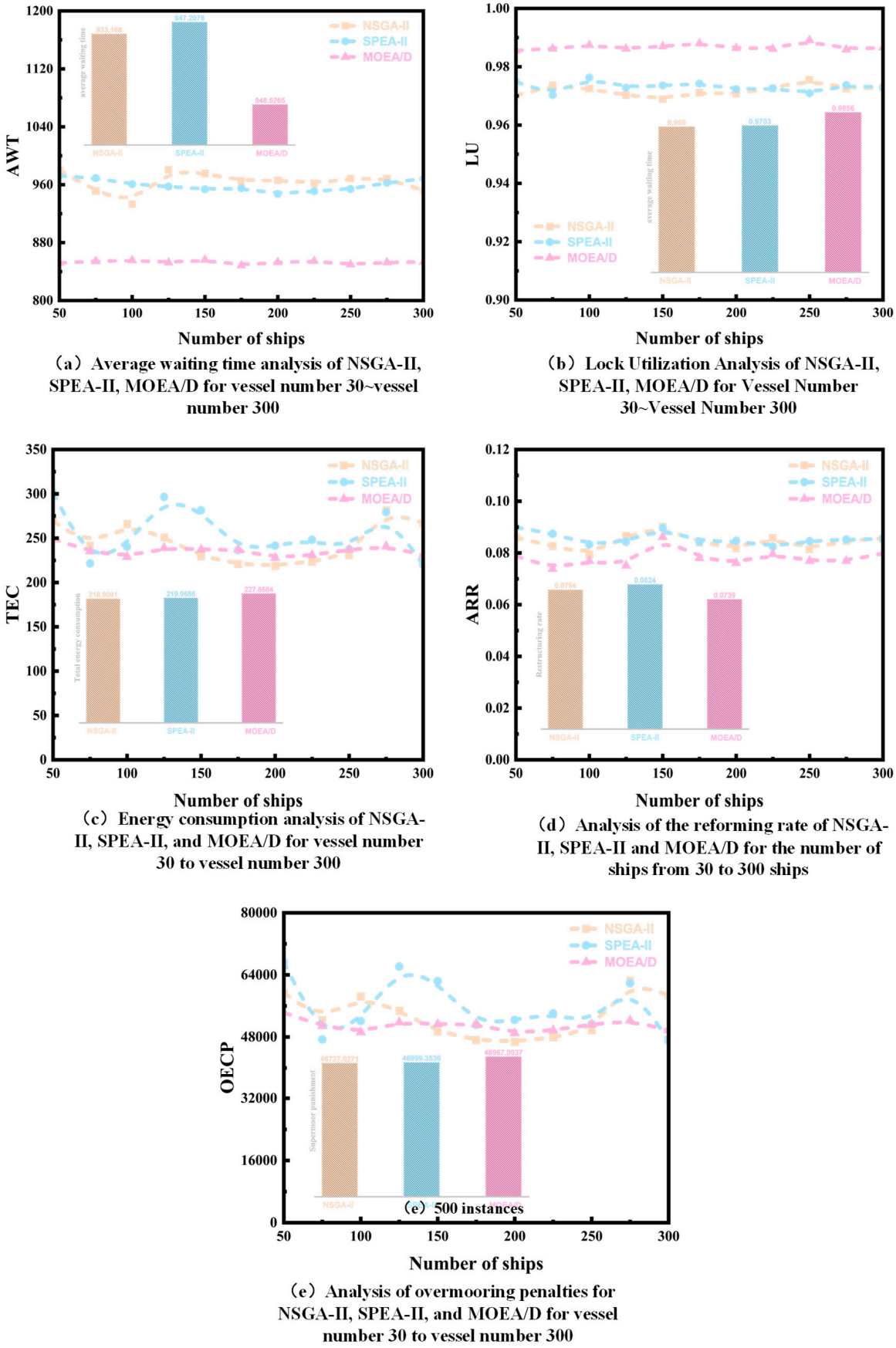
This subsection further examines algorithm performance under medium-scale inland-waterway scheduling scenarios. In comparison with the ultra-large-scale stress tests, the scenario set in Table 5 is closer to the scale of day-to-day scheduling analysis and is therefore used to evaluate how the algorithms behave under more moderate congestion levels. The discussion below emphasizes relative strengths, trade-off structures, and application suitability rather than unsupported claims of universal superiority.

Table 5. Performance comparison analysis of NSGA-II, SPEA-II and MOEA/D in ship scheduling optimization problems of different sizes.

J-N	PC														
	NSGA-II					SPEA-II					MOEA/D				
	AWT	LU	TEC	ARR	OECP	AWT	LU	TEC	ARR	OECP	AWT	LU	TEC	ARR	OECP
50 (min)	839	0.95	58	0.05	6469	837	0.95	69	0.05	9249	812	0.96	160	0.05	32,064
50 (max)	1107	0.99	506	0.11	118,511	1107	0.99	503	0.11	117,848	914	0.99	360	0.11	81,940
75 (min)	820	0.95	60	0.05	6981	822	0.95	44	0.05	2946	816	0.95	158	0.05	31,488
75 (max)	1083	0.99	438	0.11	101,524	1102	0.99	406	0.13	93,488	914	0.99	341	0.10	77,350
100 (min)	832	0.95	106	0.05	18,512	836	0.95	74	0.05	10,490	815	0.95	154	0.05	30,300
100 (max)	1050	0.99	410	0.10	94,584	1066	0.99	439	0.2	101,873	911	0.99	307	0.10	68,825
125 (min)	835	0.95	43	0.05	2810	835	0.95	103	0.05	17,729	811	0.97	126	0.05	23,386
125 (max)	1102	0.99	481	0.11	112,354	1072	0.99	480	0.11	112,065	948	0.99	364	0.10	82,969
150 (min)	828	0.95	59	0.05	6852	829	0.95	114	0.05	20,564	814	0.95	176	0.05	36,085
150 (max)	1085	0.99	449	0.12	104,231	1068	0.99	448	0.11	104,016	936	0.99	309	0.11	69,294
175 (min)	816	0.95	55	0.05	5784	815	0.95	53	0.05	5230	812	0.97	145	0.05	28,168
175 (max)	1084	0.99	421	0.11	97,270	1084	0.99	439	0.12	101,872	908	0.99	299	0.10	66,709
200 (min)	823	0.95	43	0.05	2779	817	0.95	66	0.05	8493	813	0.95	150	0.05	29,507
200 (max)	1102	0.99	430	0.12	99,417	1083	0.99	430	0.10	99,704	912	0.99	303	0.10	67,660

1. Performance Disparities and Dominant Features in Multi-objective Scheduling

As depicted in Figure 11, the three algorithms exhibit distinct optimization patterns across fleet sizes ranging from 50 to 300 ships. MOEA/D consistently performs well in waiting-time reduction and lock-utilization improvement, with AWT values of 848.53–856.08 min and LU values above 0.985 in the preserved results. However, this advantage is accompanied by comparatively higher TEC and OECP values, which suggests that MOEA/D tends to prioritize flow efficiency over energy-sensitive constraints. By contrast, SPEA-II performs relatively well on some energy-related indicators, although this is generally achieved at the cost of longer waiting time.



（a）Average waiting time analysis of NSGA-II, SPEA-II, MOEA/D for vessel number 30~vessel number 300

（b）Lock Utilization Analysis of NSGA-II, SPEA-II, MOEA/D for Vessel Number 30~Vessel Number 300

（c）Energy consumption analysis of NSGA-II, SPEA-II, and MOEA/D for vessel number 30 to vessel number 300

（d）Analysis of the reforming rate of NSGA-II, SPEA-II and MOEA/D for the number of ships from 30 to 300 ships

（e）500 instances

（e）Analysis of overmooring penalties for NSGA-II, SPEA-II, and MOEA/D for vessel number 30 to vessel number 300

Figure 11. Performance comparison of NSGA-II, SPEA-II and MOEA/D in ship scheduling optimization of different sizes.

2. Trade-off Analysis and Optimization Strategy Differences under Multi-objective Coupling

From the perspective of multi-objective balance, MOEA/D's decomposition-based strategy facilitates strong coupling between temporal and spatial efficiency, but the deterioration in energy and penalty indicators reflects intrinsic trade-offs among objectives. NSGA-II presents a more moderate balance across most indicators and retains comparatively stable arrival-rescheduling performance in the 175–300 ship range. SPEA-II shows scenario-dependent behavior: under some small- and medium-scale cases it incurs higher energy and overcapacity costs, whereas under larger cases these indicators improve to some extent, implying that its archive-maintenance mechanism adapts differently as the pressure level changes.

3. Algorithmic Suitability for Real-world Scheduling Scenarios and Future Research Directions

Based on the preserved results, algorithm selection should depend on the dominant operational requirement of the target application. For high-throughput systems, MOEA/D is attractive because of its strong space–time coordination capability, although additional energy-compensation or penalty-control mechanisms may be needed. For scenarios placing greater emphasis on energy-related objectives, SPEA-II remains a plausible option. NSGA-II is comparatively appropriate when balanced multi-objective behavior and operational stability are prioritized. Future research should consider hybrid frameworks, dynamic weight allocation, and adaptive decomposition mechanisms so that space–time efficiency and energy-related objectives can be coordinated more effectively.

5. Conclusions

Based on the historical ship lockage data from the Da Teng Gorge Ship Lock Hub, this study evaluates the behavior of four intelligent optimization algorithms—NSGA-II, NSGA-III, MOEA/D, and SPEA-II—under a ship scheduling framework involving average waiting time, lock utilization, total energy consumption, arrival-rescheduling rate, and berth-overcapacity penalty. The revised manuscript no longer claims unsupported percentage dominance in the abstract and conclusion. Instead, the preserved results indicate that NSGA-III provides the most balanced overall trade-off on the empirical instance, MOEA/D remains attractive in time-sensitive scenarios, and SPEA-II performs well in some overcapacity-control settings. The study also clarifies the physical meaning of key variables and thresholds, strengthens the operational interpretation of the reduced-order energy objective, and makes the robustness treatment more closely linked to the algorithmic search process. Because the fully archived repeated-run statistics, confidence intervals, and directly comparable rule-based baseline records are incomplete for the preserved dataset, the paper frames its findings as case-based comparative evidence rather than as definitive statistical superiority over baseline operational policies. Future research should therefore focus on stronger reproducibility through repeated-run records, explicit FCFS or priority-rule benchmarks, parameter-sensitivity testing, and online decision support under real-time disturbances.

Author Contributions: Conceptualization, Q.X.; methodology, Q.X.; validation, S.W.; formal analysis, J.W.; investigation, J.W.; resources, S.W.; data curation, H.L.; writing—original draft preparation, J.W.; writing—review and editing, S.W. and Q.Y.; visualization, H.L.; project administration, H.L.; funding acquisition, Q.X. All authors have read and agreed to the published version of the manuscript.

Funding: This research was funded by "National Natural Science Foundation of China, grant number 52362055" and "Guangxi Science and Technology Department, grant number 2025LTLT03003".

Data Availability Statement: The data presented in this study are available on request from the corresponding author.

Conflicts of Interest: Authors Qiang Yan and Song Wu were employed by the company Pinglu Canal Group Co., Ltd. The remaining authors declare that the research was conducted in the absence of any commercial or financial relationships that could be construed as a potential conflict of interest.

References

1. Wu, Z.; Ji, B.; Yu, S.S. Modeling and Solution Algorithm for Green Lock Scheduling Problem on Inland Waterways. *Mathematics* **2024**, *12*, 1192. [CrossRef]
2. Chen, K.; Guo, J.; Xin, X.; Zhang, T.; Zhang, W. Port sustainability through integration: A port capacity and profit-sharing joint optimization approach. *Ocean Coast. Manag.* **2023**, *245*, 106867. [CrossRef]
3. Liu, M.; Xin, X.; Wang, X.; Zhang, T.; Chen, K. Dual-channel slot sales strategy for container liner shipping companies with blockchain technology adoption. *Transp. Policy* **2025**, *162*, 200–220. [CrossRef]
4. Ji, B.; Yuan, X.; Yuan, Y.; Lei, X. An adaptive large neighborhood search for solving generalized lock scheduling problem: Comparative study with exact methods. *IEEE Trans. Intell. Transp. Syst.* **2019**, *21*, 3344–3356. [CrossRef]
5. Deng, Y.; Sheng, D.; Liu, B. Managing ship lock congestion in an inland waterway: A bottleneck model with a service time window. *Transp. Policy* **2021**, *112*, 142–161. [CrossRef]
6. Zhao, X.; Lin, Q.; Yu, H. A co-scheduling problem of ship lift and ship lock at the Three Gorges Dam. *IEEE Access* **2020**, *8*, 132893–132910. [CrossRef]
7. Ji, B.; Zhang, D.; Zhang, Z.; Yu, S.S.; Van Woensel, T. The generalized serial-lock scheduling problem on inland waterway: A novel decomposition-based solution framework and efficient heuristic approach. *Transp. Res. Part E Logist. Transp. Rev.* **2022**, *168*, 102935. [CrossRef]
8. Zhang, H.; Wu, Y.; Jin, Y.; Wang, S. Optimal scheduling of ships in inland waterway with serial locks. *Transp. Res. Part C Emerg. Technol.* **2025**, *178*, 105241. [CrossRef]
9. Liu, S.; Zhang, Y.; Guo, W.; Wang, W.; Zheng, Q.; Yu, H. Ship appointment scheduling for lockage operations of waterway transport with non-punctual arrivals. *Ocean Eng.* **2025**, *315*, 119844. [CrossRef]
10. Liu, S.; Zhang, Y.; Guo, W.; Tian, H.; Tang, K. Ship scheduling problem based on channel-lock coordination in flood season. *Expert Syst. Appl.* **2024**, *254*, 124393. [CrossRef]
11. Gao, P.; Xu, Z.; Huang, L.; Zhao, X. An inland waterway navigation congestion mitigation strategy based on a multi-objective moment bottleneck model. *Ocean Eng.* **2025**, *338*, 121928. [CrossRef]
12. Li, R.; Liu, Q.; Wang, L. An Index Model for the Evaluation of the Performance of Lock Navigation Scheduling Rules Considering the Perspective of Stakeholders. *Sustainability* **2024**, *16*, 2054. [CrossRef]
13. Zheng, Q.Q.; Zhang, Y.; Guo, W.; Tian, H.; Zhao, X. Solving energy-efficient lock group co-scheduling problem with ship lift and approach channel using a collaborative adaptive multi-objective algorithm. *Expert Syst. Appl.* **2024**, *242*, 122712. [CrossRef]
14. Golak, J.A.P.; Defryn, C.; Grigoriev, A. Optimizing fuel consumption on inland waterway networks: Local search heuristic for lock scheduling. *Omega* **2022**, *109*, 102580. [CrossRef]
15. Defryn, C.; Golak, J.A.P.; Grigoriev, A.; Timmermans, V. Inland waterway efficiency through skipper collaboration and joint speed optimization. *Eur. J. Oper. Res.* **2021**, *292*, 276–285. [CrossRef]
16. Jang, J.; Lim, S.; Choe, S.B.; Kim, J.S.; Lim, H.K.; Oh, J.; Oh, D. Enhanced predictive modeling vs. LCA simulation: A comparative study on CO_2 emissions from ship operations. *Ocean Eng.* **2024**, *310*, 118506. [CrossRef]
17. Tadeusz, B.; Rafal, S.; Thomas, M. Impact of trajectory simplification methods on modeling carbon dioxide emissions from ships. *Ocean Eng.* **2024**, *305*, 117905. [CrossRef]
18. Yang, X.; Gu, W.; Wang, S. Optimal scheduling of vessels passing a waterway bottleneck. *Ocean Coast. Manag.* **2023**, *244*, 106809. [CrossRef]
19. Buchem, M.; Golak, J.A.P.; Grigoriev, A. Vessel velocity decisions in inland waterway transportation under uncertainty. *Eur. J. Oper. Res.* **2022**, *296*, 669–678. [CrossRef]
20. Zhang, M.; Du, L.; Wen, Y.; Guo, L.; Guo, L.; Wu, B. Optimization of ship transport capacity structure for traffic congestion alleviation on inland waterways. *Ocean Eng.* **2024**, *311*, 118841. [CrossRef]
21. Kweon, S.J.; Hwang, S.W.; Lee, S.; Jo, M.J. Demurrage pattern analysis using logical analysis of data: A case study of the Ulsan Port Authority. *Expert Syst. Appl.* **2022**, *206*, 117745. [CrossRef]
22. Woo, S.; Yoon, S.; Kim, J.; Hwang, S.W.; Kweon, S.J. Optimal cooling shelter assignment during heat waves using real-time mobile-based floating population data. *Urban Clim.* **2021**, *38*, 100874. [CrossRef]
23. Homayouni, S.M.; de Sousa, J.P.; Moreira Marques, C. Unlocking the potential of digital twins to achieve sustainability in seaports: The state of practice and future outlook. *WMU J. Marit. Aff.* **2025**, *24*, 59–98. [CrossRef]

24. Chen, Z.; Cheng, J. Economic consequences of inland waterway disruptions in the Upper Mississippi River region in a changing climate. *Ann. Reg. Sci.* **2024**, *73*, 757–794. [CrossRef]
25. Calderón-Rivera, N.; Bartusevičienė, I.; Ballini, F. Sustainable development of inland waterways transport: A review. *J. Shipp. Trade* **2024**, *9*, 3. [CrossRef]
26. Liu, J.; Wang, Y.; Fan, N.; Wei, S.; Tong, W. A convergence-diversity balanced fitness evaluation mechanism for decomposition-based many-objective optimization algorithm. *Integr. Comput.-Aided Eng.* **2019**, *26*, 159–184. [CrossRef]
27. He, L.; Chiong, R.; Li, W.; Dhakal, S.; Cao, Y.; Zhang, Y. Multiobjective optimization of energy-efficient job-shop scheduling with dynamic reference point-based fuzzy relative entropy. *IEEE Trans. Ind. Inform.* **2022**, *18*, 600–610. [CrossRef]
28. Li, C.; Deng, L.; Qiao, L.; Zhang, L. Ensemble of neighborhood search operators for decomposition-based multi-objective evolutionary optimization. *Expert Syst. Appl.* **2025**, *277*, 127227. [CrossRef]
29. Zhu, M.; Kong, M.; Wen, Y.; Gu, S.; Xue, B.; Huang, T. A multi-objective path planning method for ships based on constrained policy optimization. *Ocean Eng.* **2025**, *319*, 120165. [CrossRef]
30. Zhang, T.; Wang, S.; Xin, X. Liner fleet deployment and slot allocation problem: A distributionally robust optimization model with joint chance constraints. *Transp. Res. Part B Methodol.* **2025**, *197*, 103236. [CrossRef]
31. Wang, X.; Zhu, H.; Luo, X.; Chang, S.; Guan, X. A novel optimal dispatch strategy for hybrid energy ship power system based on the improved NSGA-II algorithm. *Electr. Power Syst. Res.* **2024**, *232*, 110385. [CrossRef]

Disclaimer/Publisher's Note: The statements, opinions and data contained in all publications are solely those of the individual author(s) and contributor(s) and not of MDPI and/or the editor(s). MDPI and/or the editor(s) disclaim responsibility for any injury to people or property resulting from any ideas, methods, instructions or products referred to in the content.